Curcumin Enhances the Effect of Cisplatin in Suppression of Head and Neck Squamous Cell Carcinoma via Inhibition of IKKβ Protein of the NFκB Pathway

Victor M. Duarte[1,2], Eugene Han[1], Mysore S. Veena[1], Amanda Salvado[1,2], Jeffrey D. Suh[1], Li-Jung Liang[3], Kym F. Faull[4], Eri S. Srivatsan[1], and Marilene B. Wang[1,2]

Abstract

Previous experiments have shown that curcumin or cisplatin treatment suppresses growth of head and neck squamous cell carcinoma (HNSCC). To study the potential cooperative effect of both agents, two HNSCC cell lines were treated with curcumin or cisplatin alone or in combination. *In vivo* studies consisted of intravenous tail vein injection of liposomal curcumin, with intraperitoneal cisplatin, into nude mice growing xenograft HNSCC tumors. Introduction of curcumin and suboptimal concentrations of cisplatin showed a significant suppressive effect compared with treatment with either agent alone. Reduced expression of cyclin D1, IκBα, phospho-IκBα, and IKKβ occurred in cisplatin- and curcumin-treated cell lines. Confocal microscopy showed expression of IKKβ in the nucleus of the cell lines. Chromatin immunoprecipitation assay on DNA isolated from IKKβ immunoprecipitated samples showed PCR amplification of interleukin-8 promoter sequences, a binding site of NFκB, indicating an interaction between IKKβ and NFκB. Curcumin inhibited IKKβ in the cytoplasm and nucleus, leading to reduced NFκB activity, with no effect on phospho-AKT. *In vivo* studies showed significant growth inhibition of xenograft tumors treated with a combination of liposomal curcumin and cisplatin. The suppressive effect of curcumin was mediated through inhibition of cytoplasmic and nuclear IKKβ, resulting in inhibition of NFκB activity. Cisplatin treatment led to cellular senescence, indicating an effect mediated by p53 activation. The mechanisms of the two agents through different growth signaling pathways suggest potential for the clinical use of subtherapeutic doses of cisplatin in combination with curcumin, which will allow effective suppression of tumor growth while minimizing the toxic side effects of cisplatin. *Mol Cancer Ther; 9(10); 2665–75. ©2010 AACR.*

Introduction

Head and neck squamous cell carcinoma (HNSCC) is an aggressive cancer with a poor prognosis for advanced tumors. There were 40,490 new cases of HNSCC in the United States in 2006, accounting for ~3% of adult malignancies (1). The worldwide incidence exceeds half a million cases annually. The significant morbidity associated with current treatment modalities, which include disfiguring surgery, chemotherapy, and radiation, has led to continuing investigation of potential alternative and less toxic therapies.

Current treatment regimens for HNSCC include use of platinum-based chemotherapy such as cisplatin (2). Cisplatin is not effective when used as a single agent, but its efficacy is significantly enhanced when used with radiation therapy and/or in combination with other chemotherapeutic drugs. Thus, cisplatin/radiation or combination chemotherapy is the cornerstone of treatment of many cancers, including head and neck cancer. An example of this is the combination of cisplatin and cetuximab in the treatment of metastatic/recurrent head and neck cancer (3). Initial platinum responsiveness is high, but the majority of cancer patients eventually relapse with cisplatin-resistant disease. Many mechanisms of cisplatin resistance have been proposed, including changes in cellular uptake and efflux of the drug, inhibition of apoptosis, and increased DNA repair. We have hypothesized that cisplatin induces cell cycle arrest through a p16/p53-dependent pathway (4). Cisplatin has several dose-dependent side effects, including renal, otologic, and bone marrow suppression. Thus, a suboptimal level of cisplatin in combination with nontoxic agents would be useful for effective treatment of HNSCC.

Authors' Affiliations: [1]Department of Surgery, VA Greater Los Angeles Healthcare System, West Los Angeles, California and [2]Division of Head and Neck Surgery, [3]Department of Medicine, and [4]Pasarow Mass Spectrometry Laboratory, Neuropsychiatric-Semel Institute, UCLA David Geffen School of Medicine, Los Angeles, California

Note: Supplementary material for this article is available at Molecular Cancer Therapeutics Online (http://mct.aacrjournals.org/).

V.M. Duarte and E. Han contributed equally to this work.

Corresponding Author: Marilene B. Wang, Division of Head and Neck Surgery, UCLA David Geffen School of Medicine, 200 UCLA Medical Plaza Suite 550, Los Angeles, CA 90095. Phone: 310-268-3407; Fax: 310-794-7083. E-mail: mbwang@ucla.edu

doi: 10.1158/1535-7163.MCT-10-0064

Curcumin (diferuloylmethane) is the major component of the spice turmeric and is derived from the rhizome of the East Indian plant *Curcuma longa* (Fig. 1A). It has been consumed as a dietary supplement for centuries and has also been shown to prevent tumor initiation, proliferation, and metastasis in breast, colon, oral, and other human cancers (5). Curcumin is soluble only in organic solvents, but liposomal formulations have been studied in the treatment of pancreatic cancer (6).

Delivery of curcumin is limited by its poor bioavailability and insolubility in saline. Previous studies from our laboratory have shown that curcumin treatment suppresses growth of HNSCC cell lines *in vitro* and reduces tumor volume *in vivo* via topical application (7). More recently, our laboratory has shown the use of liposome-encapsulated curcumin for intravenous administration of curcumin, and bioavailability studies confirmed the presence of curcumin in circulating blood and liver (8). Its growth-inhibitory effect was mediated through the inhibition of transcription factor NFκB, resulting in the downregulation of *IκBα, cyclin D1, cyclooxygenase-2* (*COX-2*), *interleukin-6* (*IL-6*), and *interleukin-8* (*IL-8*) genes.

In the present study, we investigated whether curcumin would enhance the suppressive effect of cisplatin in HNSCC. Two HNSCC cell lines, CAL27 and UM-SCC1, were treated with curcumin and cisplatin individually or in combination. Nude mice with subcutaneous xenograft CAL27 tumors were administered with cisplatin alone or a combination of cisplatin and liposomal curcumin. In addition, the mechanism of action of curcumin, inhibiting transactivation of NFκB, mediated through cytoplasmic and nuclear IKKβ, was studied.

Materials and Methods

Cell lines

HNSCC cell lines CAL27 and UM-SCC1, representing oral cancers, were used. CAL27 was obtained from the American Type Culture Collection, and UM-SCC1 was obtained from Dr. Thomas E. Carey (University of Michigan, Ann Arbor, MI). CAL27 cells were characterized by the

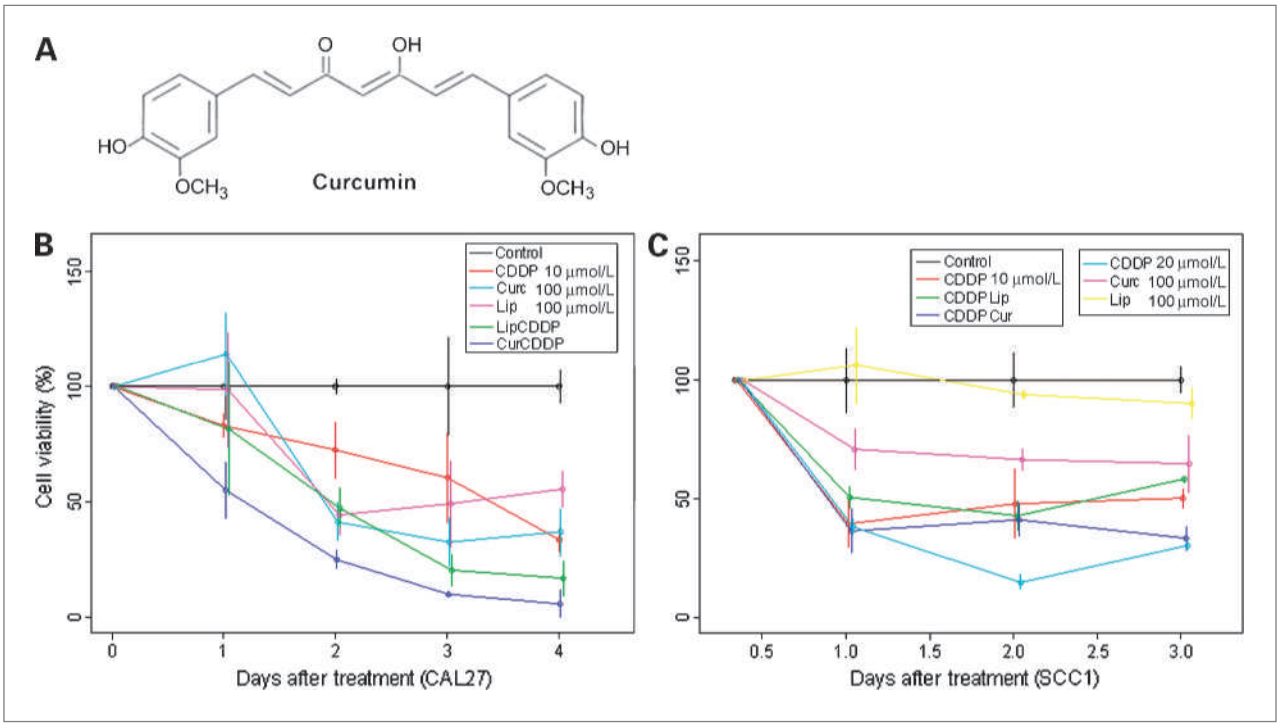

Figure 1. Growth inhibition of HNSCC *in vitro* with cisplatin and curcumin. A, molecular structure of curcumin. Cell viability by MTT assay was done on CAL27 (B) and UM-SCC1 (C) cells with cisplatin or curcumin alone or in combination. We compared the time trends (or slopes) among different groups, and the estimated slopes from the lowest to the highest in CAL27 are as follows: untreated control (0), empty liposomes (–13.89), cisplatin alone (–15.61), liposomal curcumin (–20.80), and liposomal curcumin + cisplatin (–23.35). Estimated slope values in UM-SCC1 cells are as follows: untreated control (0), empty liposomes (–4.90), curcumin (–11.46), 10 μmol/L cisplatin (–15.52), curcumin + cisplatin (–22.83), and 20 μmol/L cisplatin (–26.79). The calculations show that empty liposomes themselves have a significant growth inhibition in CAL27 cells over time (i.e., slope of growth inhibition) compared with the untreated control ($P = 0.0015$). However, the estimated slope of growth inhibition is greater with liposomal curcumin treatment in comparison with the untreated control ($P < 0.0001$). There is a significantly greater effect in liposomal curcumin–treated cells in combination with cisplatin compared with cells treated with cisplatin alone ($P = 0.0152$). Statistical significance was not observed for combination treatment of liposomal curcumin and cisplatin versus liposomes and cisplatin. In the UM-SCC1 cells, liposomal effect is minimal and a significant growth inhibition over time is seen in the presence of curcumin ($P = 0.0064$). In comparison with the untreated control, the combination treatment of curcumin with 10 μmol/L cisplatin shows an effect ($P = 0.0016$) similar to that seen with 20 μmol/L cisplatin ($P = 0.0011$).

American Type Culture Collection using polyphasic (genotypic and phenotypic) testing methods. UM-SCC1 cells were not characterized by our laboratory after receiving from the University of Michigan. Cell lines were grown in DMEM containing high glucose (4,500 μg/mL) and 1 mmol/L glutamine, 100 IU/mL penicillin, and 10% fetal bovine serum (Sigma).

Liposomal curcumin preparation

A 9:1 ratio of lipids 1,2-dimyristoyl-*sn*-glycero-3-phosphocholine and 1,2-dimyristoyl-*sn*-glycero-3-phospho-rac-(1-glycerol) (Sigma-Aldrich) was dissolved in *tert*-butanol at a concentration of 10 mg/mL. Sterile water (1/20 volume) was added and 1 part curcumin (purity, 97%; Cayman Chemical) was added for a final lipid/curcumin ratio of 10:1. The solution was sterile filtered, frozen in dry ice and acetone, and lyophilized overnight. Liposomal curcumin was suspended in sterile 0.9% NaCl at 65°C to yield a 100 mmol/L stock solution.

Curcumin and cisplatin treatment of HNSCC cell lines

Cells were plated in 24-well plates (30,000 per well) and allowed to grow for 24 hours. After serum starvation for 24 hours, cells were treated with cisplatin [10 μmol/L (i.e., 3 μg/mL) or 20 μmol/L (i.e., 6 μg/mL)] for 5 hours or with liposomal curcumin (100 μmol/L) for 8 hours. Combination treatment consisted of addition of cisplatin 3 hours after the addition of liposomal curcumin. Untreated cells or those treated with empty liposomes alone (100 μmol/L) were used as controls. Cells were then allowed to incubate in serum-containing medium at 37°C, and cell viability was measured at 24 hours. Growth assays were done at least twice and each time in triplicates.

Cell viability assay

Growth medium was aspirated out of wells and 1.0 mL of MTT solution (1 mg/mL in complete medium; Sigma-Aldrich) was added to each well. Cells were then incubated at 37°C for 4 hours. The MTT solution was aspirated out of the wells, air dried for 5 minutes, and dissolved in isopropanol, and absorbance values were read in an ELISA microplate reader at 570 nm as described (4).

Western blot analysis

Proteins were extracted from cells or xenograft tumors using radioimmunoprecipitation assay lysis buffer containing a complete protease inhibitor cocktail (Roche Diagnostics). Western blotting was done using 20 to 30 μg of denatured proteins on 4% to 20% SDS acrylamide gels (Invitrogen, Inc.). Proteins transferred onto nitrocellulose were hybridized following the established protocol (7) to the antibodies (cyclin D1, phospho-IκBα, IκBα, histone H1, and histone H3; Santa Cruz Biotechnology). All Western blot analyses were done at least twice.

Immunofluorescence

Cells were grown overnight on coverslips to semiconfluence (70–80%) and treated with liposomal curcumin for 30 minutes, 1 hour, or 4 hours. Cells were then treated with tumor necrosis factor α (TNFα) for 15 minutes. Untreated cells and cells treated with empty liposomes for 4 hours were included as controls. Immunofluorescence was done using the IKKβ, NFκB, phospho-AKT, and phospho-IκBα antibodies (Santa Cruz Biotechnology) following the established protocol (7). Confocal microscopy was done following established protocol using a Zeiss microscope.

Chromatin immunoprecipitation assay

UM-SCC1 cells grown to 80% confluency were treated with TNFα for 1 hour and cross-linked with 37% formaldehyde for 10 minutes at 37°C. Chromatin immunoprecipitation (ChIP) assays were done using ChIP Assay kit (Millipore) following the manufacturer's protocol. Immunoprecipitations were carried out using antibodies to IgG (Santa Cruz Biotechnology), IKKβ (Cell Signaling), and NFκB (Calbiochem). DNA isolated from the input as well as the immunoprecipitated samples were amplified using IL-8 and β-actin primers (9). The following primers were used in the PCR: IL-8, 5′-GGGCCATCAGTTGCAAATC-3′ (forward) and 5′-TTCCTTCCGGTGGTTTCTTC-3′ (reverse); β-actin, 5′-CAACGCCAAAACTCTCCCTC-3′ (forward) and 5′-ATCGGCAAAGGCGAGGCTCTG-3′ (reverse). DNAs were denatured at 95°C for 1 minute, annealed at 55°C for 1 minute, and extended at 72°C for 1 minute for 35 cycles. The PCR products were separated on 10% polyacrylamide gels and stained with ethidium bromide, and images were captured using the Kodak Gel documentation system.

Senescence assay

CAL27 cells grown to semiconfluence in six-well plates were treated with liposomal curcumin (100 μmol/L) for 8 hours or cisplatin (20 μmol/L) for 5 hours. Growth medium was replaced and cells were grown for 4 days. Cells were then stained with β-galactosidase, and blue senescence colonies were visualized under the microscope. Photographs were taken using a Nikon camera.

Curcumin binding studies

CAL27 cells grown to semiconfluence in 100-mm dishes were treated with liposomal curcumin (100 μmol/L) for 8 hours. After medium replacement, cells were grown for 24 hours and proteins were extracted from total cell lysates. Immunoprecipitation was done with IKKβ or phospho-S6K antibody, and the precipitate was washed five times with the cell lysate buffer. Curcumin was extracted using ethyl acetate/methanol mixture and vacuum dried, and tandem mass spectrometry (MS/MS) analysis was carried out on a triple-quadrupole spectrophotometer as described (8). Curcumin peak identification

and intensity measurement was determined using a standard curcumin run as a control. Untreated cells and cells treated with liposome alone were used as negative controls.

HNSCC xenograft tumors in mice

Five-week-old female athymic nude mice (*nu/nu*; Harlan) were used for *in vivo* experiments. Animals were injected with 2×10^6 cells in the right flank to form xenograft tumors. Animals were housed in sterile rodent microisolator caging, with filtered cage top. Two to four animals were housed in each cage, with animals resting directly on bedding. They were given free access to sterile water and food. All cages, covers, and bedding were sterilized weekly. All animal procedures were approved by the Institutional Animal Care and Use Committee of the West Los Angeles Veterans Affairs Medical Center, in accordance with the USPHS Policy on Humane Care and Use of Laboratory Animals.

Treatment of nude mice with liposomal curcumin and cisplatin

Once subcutaneous nodules were visible at the inoculation site (days 7–10 after inoculation), liposomal curcumin (50 mg/kg, 1 mg for the 20-g mouse in a maximal volume of 100 μL) or equal amount of empty liposomes was administered via tail vein injection three times a week for 4 weeks. In the fourth week, cisplatin (100 μL of 7.5 μg/mL) was administered through intraperitoneal injection. There were four groups in the study: mice with no treatment (nine), mice treated with cisplatin (seven), mice treated with empty liposomes and cisplatin (five), and mice treated with liposomal curcumin and cisplatin (six). Tumor size was measured weekly using Vernier calipers, and tumor volume was calculated using the formula $V = 4/3pW2L$, where W is half of the shorter axis diameter and L is half of the longer axis diameter as described (10). At the end of the fourth week, mice were sacrificed and tumors were removed.

Statistical analysis

For the MTT absorbance, cell viability was set to be 100% at baseline, and the percent of viable cells [(viable cell count in the experiment group/mean viable cell count) × 100] per replicate was calculated at each of the posttreatment days. To examine the differences in the reduction of cell viability over time among groups, ANOVA modeling was used with the following covariates: group, time (measured in days), and a group-by-time interaction term. The model also allows heterogeneous variance across groups.

Time trends in tumor volume among experimental groups were examined using the piecewise regression model, which allows for the trend after the injection of cisplatin at week 3 to be different from the trend before injection of cisplatin. Although mice were followed over time, their IDs were not recorded due to technical difficulties. Thus, the common repeated-measures model cannot be used in this situation. Instead, the piecewise regression model was used, with the assumption of heterogeneous variance across groups to analyze tumor volume growth. All statistical analyses were carried out with the SAS System for Windows (version 9.2)

Results

Growth inhibition of HNSCC cell lines *in vitro* with liposomal curcumin and cisplatin

Two HNSCC cell lines, CAL27 and UM-SCC1, representing aggressive oral cancers were tested for growth inhibition with cisplatin or liposomal curcumin alone or in combination. All experiments were done in triplicate in 24-well plates, and viable cell counts were measured at 24, 48, 72, and 96 hours after treatment. Empty liposomes, curcumin alone, and cisplatin alone had a significantly greater growth inhibition in CAL27 cells over time (i.e., slope of growth inhibition) compared with the untreated control ($P = 0.0015$, <0.0001, and <0.0001, respectively; Fig. 1B and C). There was significantly greater effect in liposomal curcumin–treated cells in combination with cisplatin compared with cisplatin alone–treated cells ($P = 0.0152$). Statistical significance was not observed for combination treatment of liposomal curcumin and cisplatin versus liposomes and cisplatin. In UM-SCC1 cells, liposomes alone did not show an inhibitory effect. Significant growth inhibition over time was seen in the presence of cisplatin ($P = 0.0486$ and 0.0011, for 10 and 20 μmol/L, respectively), curcumin alone ($P = 0.0064$), curcumin in combination with 10 μmol/L cisplatin ($P = 0.0016$), and liposomes in combination with 10 μmol/L cisplatin ($P = 0.0247$) compared with control. We have also observed a significantly greater effect over time in curcumin-treated cells compared with cells treated with liposomes ($P = 0.0011$). The combination treatment, liposomal curcumin and 10 μmol/L cisplatin, showed an effect similar to that seen in cells treated with 20 μmol/L cisplatin.

Reduced expression of NFκB-activated genes in curcumin and cisplatin-treated cells

We have previously shown that curcumin and cisplatin downregulate the expression of genes involved in cell cycle and apoptosis and also that cisplatin induces cellular senescence through the upregulation of p16 and p53 tumor suppressor genes (4, 7). Our studies have also shown that the effect of curcumin is mediated by the inhibition of IKKβ kinase, resulting in reduced phosphorylation of IκBα (inhibitor of NFκB) and retention of NFκB in the cytoplasm (11). Thus, cisplatin and curcumin seem to suppress cell growth through independent mechanisms.

To verify that the two agents act via different mechanisms, we did expression analysis of proteins collected from the drug-treated cell lines. Both cisplatin and curcumin showed reduced expression of cyclin D1 and phospho-IκBα in CAL27 and UM-SCC1 cell lines

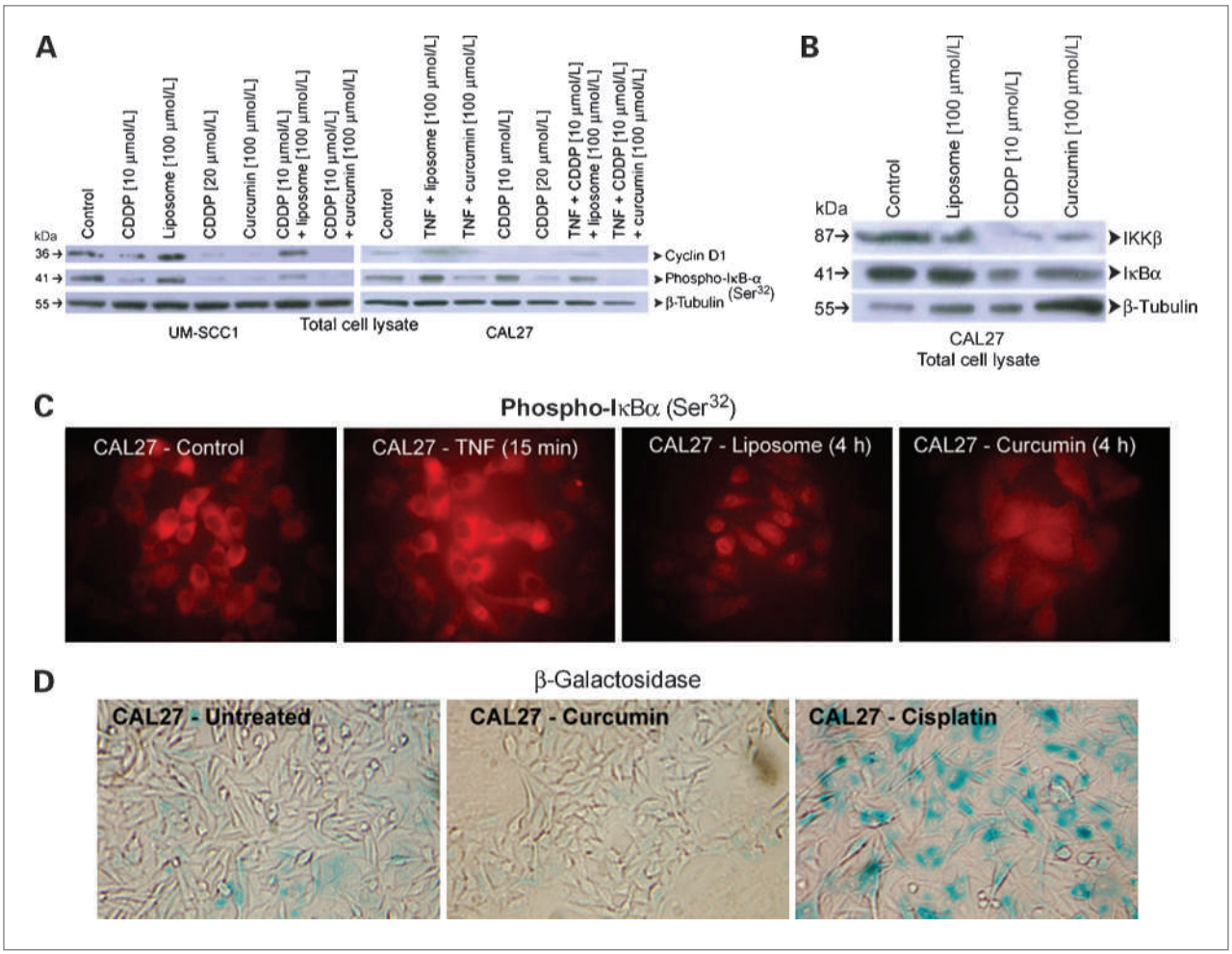

Figure 2. Inhibition of NFκB-regulated genes by cisplatin and curcumin. A, total protein lysate extracted from CAL27 and UM-SCC1 cell lines treated with cisplatin (10 or 20 μmol/L) or liposomal curcumin (100 μmol/L) or a combination of cisplatin (10 μmol/L) and liposomal curcumin (100 μmol/L) was analyzed by PAGE. Untreated cells and those treated with empty liposomes (100 μmol/L) or empty liposomes and cisplatin (10 μmol/L) served as controls. Because CAL27 cells expressed lower level of cyclin D1, cells were also pretreated with TNFα. Empty liposomes do not show any inhibitory effect on the expression of cyclin D1 or phospho-IκBα. However, reduced protein expression is observed with cisplatin or curcumin. The inhibitory effect of cisplatin-curcumin combination reaches that of 20 μmol/L cisplatin, indicating usefulness of the nontoxic curcumin as a chemotherapeutic drug for adjuvant therapy. B, hybridization of CAL27 total protein lysates to IκBα and IKKβ antibodies shows decreased expression of these two proteins in cells treated with cisplatin (10 μmol/L) or liposomal curcumin (100 μmol/L). C, immunofluorescence analysis of CAL27 cells with TNFα shows increased expression of phospho-IκBα, indicating enhanced phosphorylation through IKKβ. This expression is not affected by the addition of liposomes. However, a decrease in phospho-IκBα expression level is visualized with the addition of curcumin. D, β-galactosidase assay shows increased blue staining, indicating senescence-mediated cell death in cisplatin-treated CAL27 cells. Magnification, ×100.

(Fig. 2A). Because our previous studies have shown lower-level expression of these two proteins in CAL27 cells, in the present experiments, the cells were pretreated with TNFα for 15 minutes before the addition of drugs. A higher concentration of cisplatin (20 μmol/L) showed greater reduction in the expression of cyclin D1 and phospho-IκBα in comparison with treatment with 10 μmol/L cisplatin. In addition, combined treatment with 10 μmol/L cisplatin and liposomal curcumin resulted in greater inhibition, equaling that of treatment with 20 μmol/L cisplatin. Empty liposomes did not affect the expression of these two proteins. Western blot analysis showing reduced expression of IκBα and IKKβ in cisplatin (20 μmol/L)– and liposomal curcumin (100 μmol/L)–treated CAL27 cells (Fig. 2B) further indicated a possible direct effect on the expression of these two proteins by cisplatin and curcumin.

To confirm further that curcumin inhibited phospho-IκBα expression, immunofluorescence was done on CAL27 cells treated with liposomes or liposomal curcumin. Phospho-IκBα expression was mostly seen in the cytoplasm, and the expression level increased with the addition of TNFα (Fig. 2C). Treatment with empty liposomes resulted in increased localization of

the protein to the perinuclear region. However, curcumin treatment led to reduced protein expression in the cytoplasm and in the perinucleus of the cells, confirming the inhibitory activity of curcumin on IKK kinase, resulting in decreased phosphorylation of IκBα.

To show that cisplatin inhibits cell growth through a senescence pathway, CAL27 cells treated with liposomal curcumin or cisplatin were stained for the expression of β-galactosidase, a marker for cellular senescence. Untreated cells contained a low-level background blue staining due to cell death from confluent cell culture in 4 days of study protocol (Fig. 2D). Although there was cell killing in curcumin-treated cells, there was no observable blue stain, indicating a senescence-independent cell death by liposomal curcumin. As expected, cisplatin-treated cells showed a high-level expression of β-galactosidase, correlating to senescence-mediated cell death of HNSCC cells.

Curcumin binds to IKKβ protein subunit of the IKK complex

Because we have previously shown that curcumin inhibited IKK kinase activity (11), we did MS/MS analysis to determine whether there was a direct binding of curcumin to IKKβ protein. Cell lysates of CAL27 treated with curcumin were immunoprecipitated with IKKβ or a control phospho-S6K antibody, and the antibody-bound products were extracted with organic solvents. Analysis by MS showed the presence of curcumin peak in the cell lysates. Intensity measurements using a curcumin standard showed a 5-fold increased binding of curcumin to IKKβ in comparison with phospho-S6K (Supplementary Table S1), indicating an interaction between curcumin and IKKβ.

Nuclear expression of IKKβ protein in HNSCC cell lines

To verify further whether curcumin binding resulted in the inhibition of IKKβ expression as was seen in Western blotting, confocal microscopy was done. We observed expression of IKKβ both in the cytoplasm and in the nucleus of CAL27 and UM-SCC1 cell lines (Fig. 3A). Although the nuclear presence of the IKKα protein has been shown before (12), there is only one recent report indicating the expression of IKKβ protein in the nucleus of normal and neoplastic B lymphocytes (9). Thus, for the first time, we have seen IKKβ expression in the nucleus of HNSCC cell lines. To confirm this finding, we used two different IKKβ antibodies and HeLa cells, a cervical cancer cell line shown before to contain cytoplasmic IKKβ expression. Expression of IKKβ in HeLa cells was seen in the cytoplasm as well as in the nucleus of the cells (Fig. 3A). Costaining with 4′,6-diamidino-2-phenylindole (DAPI; left column), a nuclear-specific stain, showed magenta staining of the nucleus (last column in Fig. 3A), confirming nuclear expression of IKKβ in HeLa and HNSCC cell lines. Whereas treatment with liposomes did not have an effect on the expression of IKKβ, liposomal curcumin treatment resulted in an inhibitory effect both in the cytoplasmic and in the nuclear expression of this protein (last row in Fig. 3A). As a confirmation to cytoplasmic and nuclear localization of IKKβ, we did confocal microscopy for nuclear-specific proteins histones H1 and H3. The results showed complete localization of histone H1 to the nucleus (Fig. 3B). Expression of histone H3 was seen as speckles inside the nucleus as wells in the perinuclear/cytoplasmic region (Fig. 3B). Western blot hybridization studies of the cytoplasmic and nuclear extracts of CAL27 and HeLa cells further confirmed the presence of IKKβ in the nucleus of these two cell lines (Fig. 3C). Immunoprecipitation with nuclear IKKβ from CAL27 cells and hybridization to histone H3 antibody showed binding of histone H3, indicating a role for nuclear IKKβ in chromatin remodeling (Fig. 3C). There was also hybridization to NFκB in these immunoblots, indicating an interaction between NFκB and IKKβ proteins in the cytoplasm as well as in the nucleus. These interactions were confirmed by the hybridization of IKKβ antibody to the immunoprecipitates of cytoplasmic and nuclear NFκB (Fig. 3C). Finally, ChIP assay showed amplification of IL-8 promoter sequences (NFκB binding site) in the DNA isolated from the IKKβ antibody immunoprecipitated samples, indicating an interaction between IKKβ and NFκB (Fig. 3D). IL-8 promoter amplification was not seen with the IgG antibody precipitated samples used as a control. There was no amplification of β-actin promoter sequences in any of the immunoprecipitated samples again used as a control in the ChIP assay.

To verify the effect of curcumin on nuclear IKKβ and on NFκB, liposome- and liposomal curcumin–treated CAL27 cells were studied by immunofluorescence. Expression was also measured with the addition of TNFα, a NFκB upregulating molecule. IKKβ expression was seen in the nucleus, and there was a minimal effect with the addition of TNFα (Fig. 4A). Treatment with liposome did not alter the expression. However, reduced expression was observed in as little as 30 minutes after curcumin treatment. The presence of IKKβ in nucleosome-like particles again showed a possible role of this protein in chromatin remodeling. Expression of NFκB was seen in the cytoplasm, and increased nuclear transport occurred with the addition of TNFα (Fig. 4B). NFκB expression in liposome-treated cells resembled that of control cells. Reduction in the expression of NFκB could be seen in curcumin-treated cells. However, the inhibitory effect was pronounced with the blockage of NFκB transport in the presence of TNFα, confirming the inhibitory effect of curcumin on the transcriptional activation of NFκB. Here, the results clearly show the effect of curcumin on cytoplasmic IKKβ, leading to the inhibition of IKKβ kinase activity. Finally, we did not see an inhibitory effect on phospho-AKT expression in the presence or absence of TNFα (Fig. 4C), confirming our previous finding that curcumin inhibited NFκB by an AKT-independent mechanism in HNSCC cells.

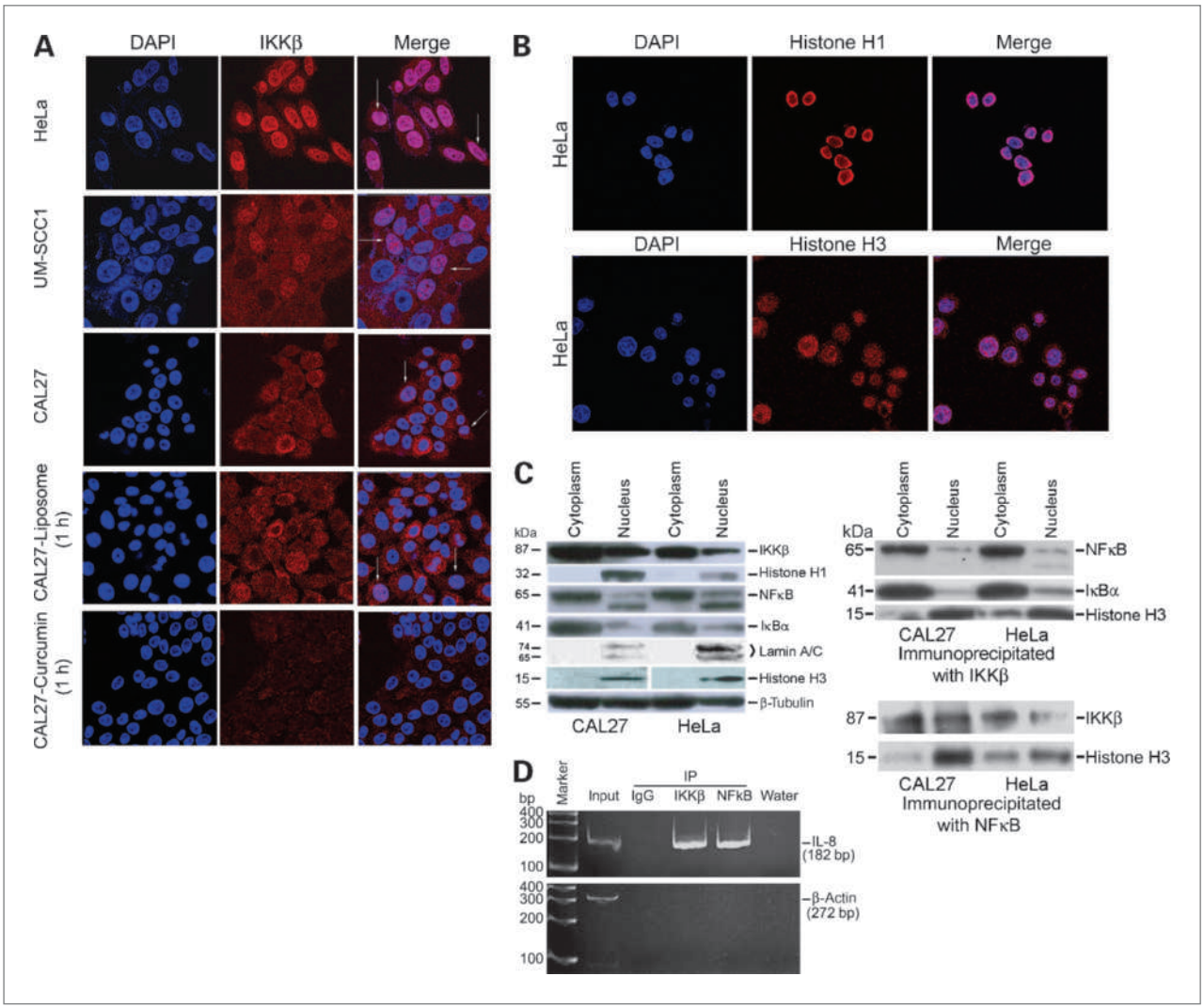

Figure 3. Nuclear expression of IKKβ in HNSCC cell lines. A, confocal microscopy with a Zeiss microscopic system done on HeLa, CAL27, and UM-SCC1 cells shows cytoplasmic and nuclear localization of IKKβ in all three cell lines. However, nuclear expression is more prominent in HeLa and UM-SCC1 cell lines. Costaining with DAPI shows magenta staining of the nuclei, confirming nuclear localization of IKKβ in all three cell lines. Cytoplasmic staining is also visualized in these photographs. Whereas treatment with liposomes does not affect the expression of IKKβ in CAL27 cells, treatment with liposomal curcumin results in reduced expression of the protein in the nucleus and cytoplasm (last row). Arrows point to nuclear magenta staining indicating costaining of DAPI and IKKβ. Magnification, ×63. B, confocal microscopy on HeLa cells shows nuclear expression of histones H1 and H3. Costaining with DAPI indicates the presence of a small fraction of histone H3 in the perinuclear/cytoplasmic region. Speckle-like staining of histone H3 could indicate localization to nucleosomes involved in chromatin remodeling. C, Western blot analysis of cytoplasmic and nuclear fractions of CAL27 and HeLa cells with IKKβ shows the presence of IKKβ in both the cell compartments. Whereas histones H1 and H3 and lamin A/C used as controls represent proteins of the nucleus, β-tubulin is present both in the cytoplasm and in the nucleus. Immunoprecipitation with IKKβ antibody followed by Western blot analysis shows predominant binding of nuclear histone H3 to IKKβ, indicating a role for IKKβ in chromatin remodeling. Minor hybridization seen in the cytoplasmic fraction could represent hybridization to the cytoplasmic H3 protein. Binding of nuclear IKKβ to NFκB is also seen in the immunoblots. The cytoplasmic IKKβ binds to NFκB and IκBα, confirming its role in the phosphorylation and ubiquitination of IκBα. The interaction between NFκB and IKKβ in the nucleus and cytoplasm is confirmed by the immunoprecipitation of proteins with NFκB antibody followed by hybridization to IKKβ. D, ChIP assay done on DNA isolated from IKKβ and NFκB immunoprecipitated samples shows a PCR product of 182 bp for IL-8 promoter sequences. PCR product is not seen in the IgG immunoprecipitated sample. Whereas the input DNA is positive for the 272-bp β-actin promoter sequence, the immunoprecipitated samples do not show the PCR product, confirming the specificity of the ChIP assay.

Enhanced growth inhibition of *in vivo* xenograft tumors with combination (liposomal curcumin and cisplatin) therapy

CAL27 xenograft tumors were grown in nude mice, and tumor dimensions were measured weekly with calipers. Once it was evident that xenograft tumors were forming (7 days), liposomes and liposomal curcumin in saline were injected via the tail vein three times a week for 4 weeks. In the fourth week, mice also received cisplatin by intraperitoneal injection. A

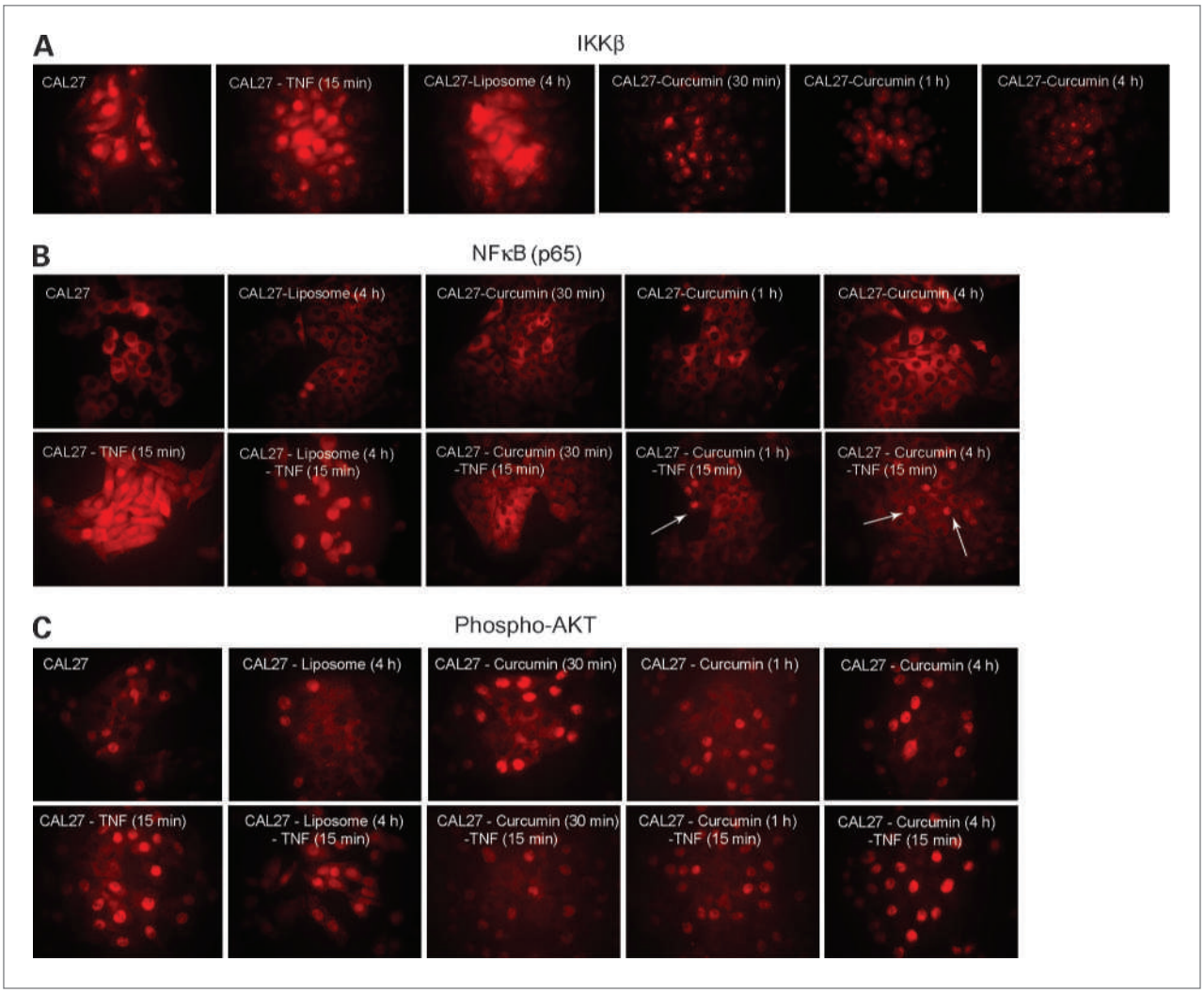

Figure 4. Confirmation of IKKβ protein expression in the nucleus. A, immunofluorescence studies show inhibition of nuclear IKKβ with a 30-min curcumin treatment and the inhibition is greater for longer treatments. The speckle-like particles possibly represent nucleosomes involved in chromatin remodeling. B, NFκB is mostly localized to the cytoplasm and is transported to the nucleus with the addition of TNFα. Whereas there is no difference in NFκB expression in liposome-treated cells, curcumin-treated cells show inhibition of nuclear transport, and this inhibition is clearly visible after the addition of TNFα. C, the absence of an effect on phospho-AKT points to an AKT-independent downregulation of NFκB by curcumin. Arrows indicate cells with nuclear expression. Magnification, ×100.

slower tumor growth rate of liposomal curcumin–treated mice for the first 3 weeks confirmed our earlier findings (8). Results from the piecewise regression model indicated that in comparison with the control, a greater inhibitory effect over time (i.e., estimated slope of growth) was seen with the curcumin-cisplatin combination treatment before and after receiving cisplatin. However, the estimated difference in slopes of growth did not reach statistical significance (P = 0.1098). A box plot is a convenient way of graphically depicting groups of numerical data through their five-number summaries (minimum, lower quartile, median, upper quartile, and maximum). The tumor volume over the first 3 weeks for cisplatin alone (Fig. 5B, top right) and curcumin-cisplatin (Fig. 5B, bottom right) did not go beyond 100 mm (Fig. 5B, dashed lines), except one observation at week 3 in the cisplatin alone group. In addition, a smaller variation in tumor volume is seen 1 week after the injection of cisplatin (week 4) for these two groups. This analysis again showed growth inhibition of xenograft tumors in the combination treatment in comparison with cisplatin alone or the controls (Fig. 5B). The tumor size shown in Fig. 5C showed growth inhibition with cisplatin alone and an enhanced growth reduction with the inclusion of curcumin in the combination treatment. Western blot analysis showed a marginal inhibitory effect on the expression of cyclin D1 in cisplatin-treated tumors (Fig. 5D). However, liposomal curcumin treatment in combination with cisplatin resulted in a

marked decrease in cyclin D1 expression correlating to the inhibitory effect on tumor growth.

Discussion

The mechanism of action of cisplatin includes cell cycle arrest and initiation of apoptosis (13). We and others have shown that cisplatin induces cellular senescence through activation of p53 and p16 proteins, and there is strong evidence that p53 plays a role in cisplatin sensitivity. It also seems that cisplatin-induced growth arrest in human cancer cells has characteristics of senescence in addition to apoptosis (14). In the present investigation, we used HNSCC cell lines containing mutated p53 and lacking p16 expression. The senescence-associated β-galactosidase activity was seen in the CAL27 cells following cisplatin exposure, suggesting that growth of cancer cells containing mutated p53 function can also be inhibited by cisplatin via nuclear transportation of p53 protein (4). Previous results further suggest that functional expression of p16 augments the effect of cisplatin in cell killing. Because p16 and p53 are functionally active in the nucleus, it is likely that cisplatin plays an essential role in the nuclear transport and stabilization of these proteins for cell cycle arrest and apoptosis. We have shown here that in the presence of cisplatin, there is reduced expression of NFκB-regulated proteins cyclin D1 and phospho-IκBα, thereby indicating control of NFκB transactivation by cisplatin through the nuclear p53 protein.

Tumor cells evade apoptosis by downregulation of apoptotic proteins and upregulation of antiapoptotic proteins. Expression of growth signaling pathways gives them survival advantage and allows them to resist therapy-induced apoptosis (15). We and others have shown that curcumin-mediated head and neck cancer cell growth inhibition occurs through the inhibition of NFκB activity (8, 16–18). Recently, we have reported that the inhibitory effect of curcumin on NFκB is by the inhibition of IKK

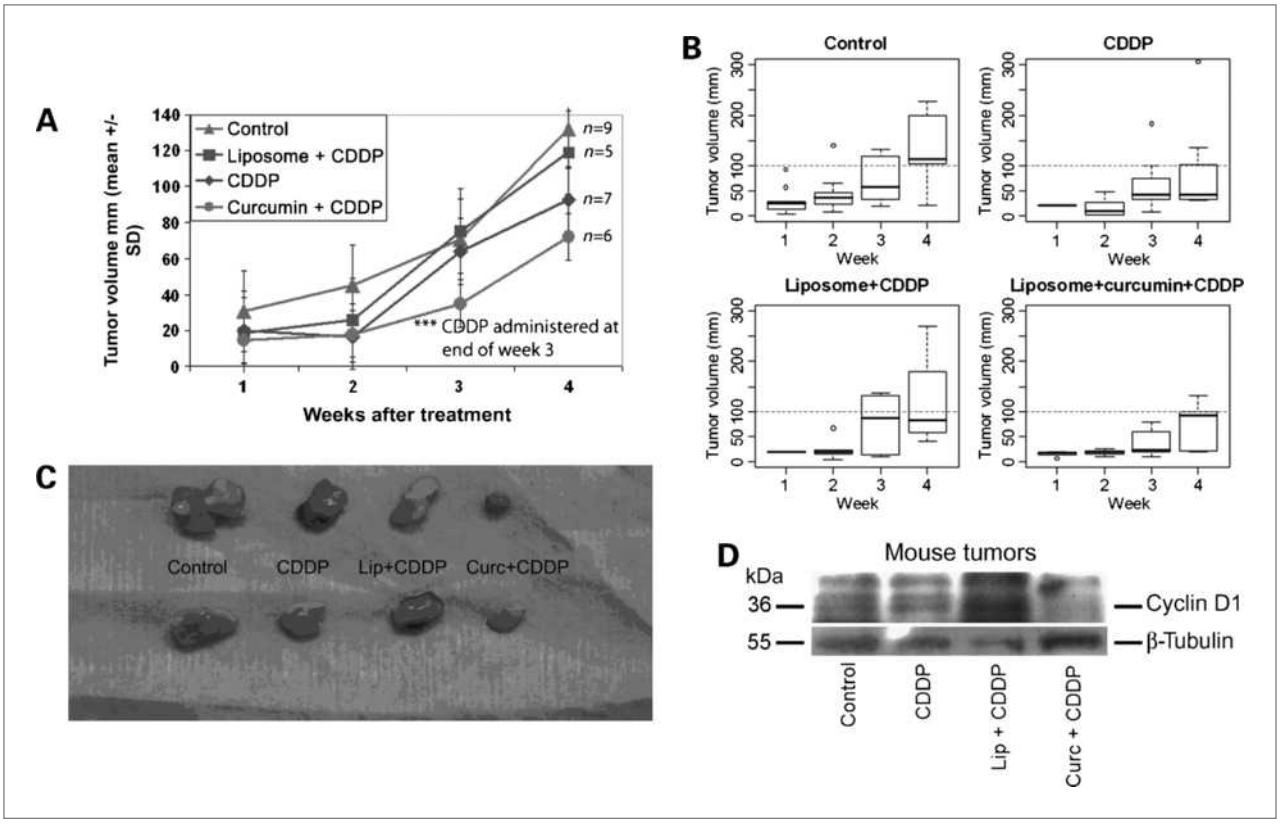

Figure 5. Inhibition of CAL27 mouse xenograft tumors with cisplatin or cisplatin-curcumin combination. Mice were treated with empty liposomes or liposomal curcumin for 3 wk after the appearance of tumor nodules. Intraperitoneal injection of cisplatin was administered on the fourth week, and a week later, tumors were excised. A, tumor volume was calculated using the method described in Materials and Methods. Compared with control, the results show tumor growth inhibition with cisplatin treatment. A greater inhibitory effect was seen with the curcumin-cisplatin combination treatment before and after receiving the cisplatin. However, the estimated difference in slopes of growth between the curcumin-cisplatin combination and control did not reach statistical significance ($P = 0.1098$). B, a box plot is a convenient way of graphically depicting groups of numerical data through their five-number summaries (minimum, lower quartile, median, upper quartile, and maximum). The analysis shows reduced growth of the xenograft tumors in the combination treatment in comparison with other groups. C, representative tumors show reduced growth with cisplatin treatment and greater tumor growth inhibition with the cisplatin-curcumin combination treatment. D, Western blot analysis of proteins isolated from the xenograft tumors shows a marginal reduction in cyclin D1 expression in cisplatin-treated tumors in comparison with the untreated controls. However, treatment with the combination of cisplatin and curcumin shows significant reduction in the expression of cyclin D1, correlating to tumor size reduction in the combination treatment.

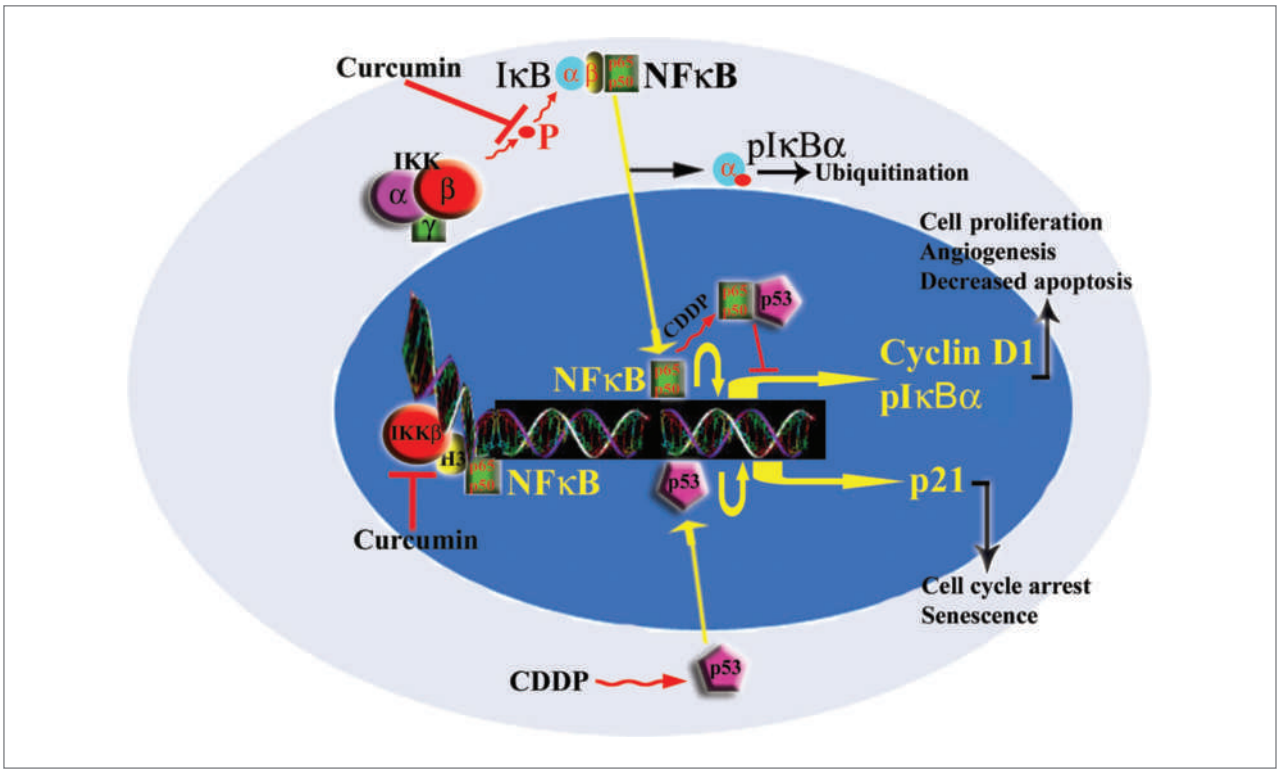

Figure 6. Mechanism of action of curcumin and cisplatin. The available data suggest NFκB activation to be inhibited through a p53-directed mechanism by cisplatin. Inhibition of NFκB seems to occur through the downregulation of IKKβ by curcumin. Histone H3 (H3) bound to IKKβ, forming a nucleosomal complex.

kinase (11). In the present investigation, we have shown that this inhibition could be due to direct interaction between curcumin and IKKβ. Further, for the first time, we have shown the presence of IKKβ in the nucleus whose function seems to be related to transcriptional activation of NFκB by chromatin remodeling. Additional studies including ChIP assay will be required to determine the proteins recruited by IKKβ for this NFκB transactivation.

Transcription factor NFκB and the serine/threonine kinase AKT play critical roles in cancer cell survival and have been shown to be activated in various malignancies (19, 20). Some have shown that curcumin acts via an AKT-dependent pathway in cell growth regulation (21, 22). Previous studies in our laboratory revealed that liposomal curcumin treatment suppressed the activation of NFκB without affecting the expression of phospho-AKT or its downstream target phospho-S6 kinase (8). Here, we have confirmed using immunofluorescence that curcumin affects NFκB expression via an AKT-independent mechanism.

Recent investigative trials include gene-targeted therapies in HNSCC, including cetuximab, bevacizumab, and erlotinib, targeted against epidermal growth factor receptor (EGFR; refs. 23–27). Although anti-EGFR therapies are active in some patients, eventually disease in nearly all patients will become refractory to therapy (28). Mutations in the EGFR receptor seem to play a significant role in the resistance to EGFR therapy. Thus, efforts are under way to identify alternate therapies, including the use of curcumin in combination with radiation and/or chemotherapeutic drugs in hepatic carcinoma, ovarian carcinoma, and HNSCC (29–31).

In conclusion, we have used the combination of curcumin and cisplatin to show enhanced growth suppression in HNSCC. We believe that this occurs through two different molecular pathways. Curcumin affects NFκB transactivation by inhibiting IKK kinase activity both in the cytoplasm and in the nucleus, possibly through an interaction with IKKβ (Fig. 6). We hypothesize that nuclear IKKβ in combination with histone H3 is involved in chromatin remodeling of the NFκB transcription binding sites. Inhibition of IKKβ by curcumin therefore results in reduction in NFκB-occupied sites in chromatin, leading to a decrease in NFκB-mediated transcription. Cisplatin, in contrast, downregulates NFκB through a p53-mediated pathway. We therefore believe that the therapeutic potential of cisplatin will be enhanced with the addition of curcumin, with lower, less toxic doses of cisplatin required for its cytotoxic effect.

Disclosure of Potential Conflicts of Interest

No potential conflicts of interest were disclosed.

Acknowledgments

We thank Dr. Yasutada Akiba for confocal microscopy and Dr. Ke Wei Zhao for help in acquiring photographic images.

Grant Support

VA Greater Los Angeles Healthcare, West Los Angeles Surgical Education Research Center, and UCLA Academic Senate (M.B. Wang); NIH grant R21 CA116826-01 (M.B. Wang); and Veterans Administration (Washington, DC) Merit grant (E.S. Srivatsan).

The costs of publication of this article were defrayed in part by the payment of page charges. This article must therefore be hereby marked *advertisement* in accordance with 18 U.S.C. Section 1734 solely to indicate this fact.

Received 01/27/2010; revised 08/04/2010; accepted 08/08/2010; published OnlineFirst 10/11/2010.

References

1. Jemal A, Siegel R, Ward E, et al. Cancer statistics, 2006. CA Cancer J Clin 2006;56:106–30.
2. Stordal B, Davey R. A systematic review of genes involved in the inverse resistance relationship between cisplatin and paclitaxel chemotherapy: role of BRCA1. Curr Cancer Drug Targets 2009;9:354–65.
3. Burtness B, Goldwasser M, Flood W, et al. Phase III randomized trial of cisplatin plus placebo compared with cisplatin plus cetuximab in metastatic/recurrent head and neck cancer: an Eastern Cooperative Oncology Group study. J Clin Oncol 2005;23:8646–54.
4. Yip HT, Chopra R, Chakrabarti R, et al. Cisplatin-induced growth arrest of head and neck cancer cells correlates with increased expression of p16 and p53. Arch Otolaryngol Head Neck Surg 2006;132:317–26.
5. Reuter S, Eifes S, Dicato M, et al. Modulation of anti-apoptotic and survival pathways by curcumin as a strategy to induce apoptosis in cancer cells. Biochem Pharmacol 2008;76:1340–51.
6. Li L, Braiteh FS, Kurzrock R, et al. Liposome-encapsulated curcumin: *in vitro* and *in vivo* effects on proliferation, apoptosis, signaling, and angiogenesis. Cancer 2005;104:1322–31.
7. LoTempio M, Veena MS, Steele H, et al. Curcumin suppresses growth of head and neck squamous cell carcinoma. Clin Cancer Res 2005;11:6994–7002.
8. Wang D, Veena MS, Stevenson K, et al. Liposome-encapsulated curcumin suppresses growth of head and neck squamous cell carcinoma *in vitro* and in xenografts through the inhibition of nuclear factor κB by an AKT-independent pathway. Clin Cancer Res 2008;14:6228–36.
9. Fu L, Lin-Lee YC, Pham LV, Tamayo AT, Yoshimura LC, Ford RJ. BAFF-R promotes cell proliferation and survival through interaction with IKKβ and NF-κB/c-Rel in the nucleus of normal and neoplastic B-lymphoid cells. Blood 2009;113:4627–36.
10. Kunnumakkara AB, Diagaradjane P, Guha S, et al. Curcumin sensitizes human colorectal cancer xenografts in nude mice to γ-radiation by targeting nuclear factor-κB-regulated gene products. Clin Cancer Res 2008;14:2128–36.
11. Cohen A, Veena MS, Srivatsan ES, et al. Suppression of IL-6 and IL-8 production in head and neck cancer cells with curcumin via inhibition of Iκβ kinase (IKK). Arch Otolaryngol Head Neck Surg 2009;135:190–7.
12. Anest V, Hanson JL, Cogswell PC, et al. A nucleosomal function for IκB kinase-α in NF-κB-dependent gene expression. Nature 2003; 423:659–63.
13. Kartalou M, Essigmann JM. Mechanisms of resistance to cisplatin. Mutat Res 2001;478:23–43.
14. Rebbaa A, Zheng X, Chu F, Mirkin BL. The role of histone acetylation versus DNA damage in drug-induced senescence and apoptosis. Cell Death Differ 2006;13:1960–7.
15. Karunagaran D, Rashmi R, Kumar TR. Induction of apoptosis by curcumin and its implications for cancer therapy. Curr Cancer Drug Targets 2005;5:117–29.
16. Jobin C, Bradham CA, Russo MP, et al. Curcumin blocks cytokine-mediated NF-κB activation and proinflammatory gene expression by inhibiting inhibitory factor I-κB kinase activity. J Immunol 1999;163: 3474–83.
17. Lin YG, Kunnumakkara AB, Nair A, et al. Curcumin inhibits tumor growth and angiogenesis in ovarian carcinoma by targeting the nuclear factor-κB pathway. Clin Cancer Res 2007;13:3423–30.
18. Li L, Ahmed B, Mehta K, Kurzrock R. Liposomal curcumin with and without oxaliplatin: effects on cell growth, apoptosis, and angiogenesis in colorectal cancer. Mol Cancer Ther 2007;6: 1276–82.
19. Van Waes C. Nuclear factor-κB in development, prevention, and therapy of cancer. Clin Cancer Res 2007;13:1076–82.
20. Pugazhenti S, Akhov L, Selvaraj G, et al. Regulation of heme oxygenase-1 expression by demethoxy curcumoids through Nrf2 by a PI3-kinase/Akt mediated pathway in mouse B-cells. Am J Physiol Endocrinol Metab 2007;293:E645–55.
21. Tomita M, Matsuda T, Kawakami H, et al. Curcumin targets Akt cell survival signaling pathway in HTLV-1-infected T-cell lines. Cancer Sci 2006;97:322–7.
22. Aoki H, Takada Y, Kondo S, et al. Evidence that curcumin suppresses the growth of malignant gliomas *in vitro* and *in vivo* through induction of autophagy: role of Akt and extracellular-signal regulated kinase signaling pathways. Mol Pharmacol 2007;72:29–39.
23. Lin C, Calvo E, Papadopolus K, et al. Phase I study of cetuximab, erlotinib, and bevacizumab in patients with advanced solid tumors. Cancer Chemother Pharmacol 2009;63:1065–71.
24. Laimer K, Spizzo G, Gastl G, et al. High EGFR expression predicts poor prognosis in patients with squamous cell carcinoma of the oral cavity and oropharynx: a TMA-based immunohistochemical analysis. Oral Oncol 2007;43:193–8.
25. Agra IM, Carvalho AL, Pinto CA, et al. Biological markers and prognosis in recurrent oral cancer after salvage surgery. Arch Otolaryngol Head Neck Surg 2008;134:743–9.
26. William WN, Kim ES, Herbst RS. Cetuximab therapy for patients with advanced squamous cell carcinomas of the head and neck. Nat Clin Pract Oncol 2009;6:132–3.
27. Lilenbaum R, Axelrod R, Thomas S, et al. Randomized phase II trial of erlotinib or standard chemotherapy in patients with advanced non-small-cell lung cancer and a performance status of 2. J Clin Oncol 2008;26:863–9.
28. Harandi A, Zaidi A, Stocker A, et al. Clinical efficacy and toxicity of anti-EGFR therapy in common cancers. J Oncol 2009;2009: 1–14.
29. Nortarbartolo M, Poma P, Perri D, et al. Antitumor effects of curcumin, alone, or in combination with cisplatin or doxorubicin, on human hepatic cancer cells. Analysis of their possible relationship to changes in NF-κB activation levels and in IAP gene expression. Cancer Lett 2005;224:53–65.
30. Chirnomas D, Taniguchi T, De La Vega M, et al. Chemosensitization to cisplatin by inhibitors of the Fanconi anemia/BRCA pathway. Mol Cancer Ther 2006;5:952–61.
31. Khafif A, Lev-Ari S, Vexler A, et al. Curcumin: a potential radioenhancer in head and neck cancer. Laryngoscope 2009;119: 2019–26.